University Library

MINERVA ACCESS

A gateway to Melbourne's research publications

Minerva Access is the Institutional Repository of The University of Melbourne

Author/s:
Marzec, KM;Perez-Guaita, D;De Veij, M;McNaughton, D;Baranska, M;Dixon, MWA;Tilley, L;Wood, BR

Title:
Red blood cells polarize green laser light revealing hemoglobin's enhanced non-fundamental Raman modes

Date:
2014-10-20

Citation:
Marzec, K. M., Perez-Guaita, D., De Veij, M., McNaughton, D., Baranska, M., Dixon, M. W. A., Tilley, L. & Wood, B. R. (2014). Red blood cells polarize green laser light revealing hemoglobin's enhanced non-fundamental Raman modes. Chemphyschem, 15 (18), pp.3963-3968. https://doi.org/10.1002/cphc.201402598.

Persistent Link:
https://hdl.handle.net/11343/123794

License:
CC BY-NC

ChemPubSoc Europe

DOI: 10.1002/cphc.201402598

# Red Blood Cells Polarize Green Laser Light Revealing Hemoglobin's Enhanced Non-Fundamental Raman Modes

Katarzyna M. Marzec,[a, c] David Perez-Guaita,[a, b] Marleen de Veij,[a] Don McNaughton,[a] Malgorzata Baranska,[c, d] Matthew W. A. Dixon,[e] Leann Tilley,[e] and Bayden R. Wood*[a]

In general, the first overtone modes produce weak bands that appear at approximately twice the wavenumber value of the fundamental transitions in vibrational spectra. Here, we report the existence of a series of enhanced non-fundamental bands in resonance Raman (RR) spectra recorded for hemoglobin (Hb) inside the highly concentrated heme environment of the red blood cell (RBC) by exciting with a 514.5 nm laser line. Such bands are most intense when detecting parallel-polarized light. The enhancement is explained through excitonic theory invoking a type C scattering mechanism and bands have been assigned to overtone and combination bands based on symmetry arguments and polarization measurements. By using malaria diagnosis as an example, we demonstrate that combining the non-fundamental and fundamental regions of the RR spectrum improves the sensitivity and diagnostic capability of the technique. The discovery will have considerable implications for the ongoing development of Raman spectroscopy for blood disease diagnoses and monitoring heme perturbation in response to environmental stimuli.

## 1. Introduction

Resonance Raman (RR) spectroscopy has long been applied to monitoring the molecular dynamics of hemoglobin (Hb).[1–3] This highly symmetric and chromophoric heme prosthetic group provides strong resonance enhancement, especially when in resonance with the intense electronic transitions centered at approximately 400 nm (Soret or B band), 525 nm ($Q_v$ or α band), and 575 nm ($Q_0$ or β band)[4,5] (Figure 1).

When the laser wavelength interacts with heme groups in resonance with electronic transitions of the Soret band, the A-term scattering mechanism dominates. In A-term scattering, also known as Franck–Condon (FC) scattering, only totally symmetric modes are enhanced. Non-FC dependence of the electronic transition moment on the vibrational coordinate is possible through B-term and C-term enhancement.[6] When the excitation is in resonance with the weaker $Q_0$ band at approxi-

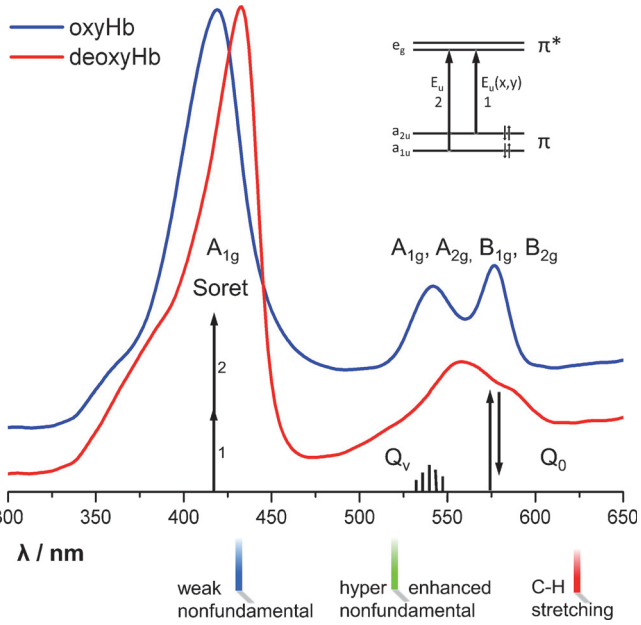



**Figure 1.** Comparison between average UV/Vis electronic absorption spectra collected from ten different oxygenated and deoxygenated RBCs in the spectral regions of 300–650 nm. Figure shows the allowed electronic transitions based on the Gouterman four-orbital model along with the laser lines used in this experiment (color coded) and the symmetry terms of the bands that are enhanced at the three major electronic transitions.

[a] Dr. K. M. Marzec, Dr. D. Perez-Guaita, Dr. M. de Veij, Prof. D. McNaughton, Prof. B. R. Wood
Centre for Biospectroscopy, School of Chemistry
Monash University, Clayton, VIC, 3800 (Australia)
E-mail: bayden.wood@monash.edu

[b] Dr. D. Perez-Guaita
Analytical Chemistry Department
University of Valencia, 46–100, Dr. Moliner 50, Burjassot (Spain)

[c] Dr. K. M. Marzec, Prof. M. Baranska
Jagiellonian Centre for Experimental Therapeutics
Jagiellonian University, Bobrzynskiego 14, 30–348 Krakow (Poland)

[d] Prof. M. Baranska
Faculty of Chemistry
Jagiellonian University, Ingardena 3, 30–060 Krakow (Poland)

[e] Dr. M. W. A. Dixon, Prof. L. Tilley
Department of Biochemistry and Molecular Biology, Bio21 Institute and ARC Centre of Excellence for Coherent X-Ray Science
The University of Melbourne, Victoria 3010 (Australia)

Supporting Information for this article is available on the WWW under http://dx.doi.org/10.1002/cphc.201402598.

© 2014 The Authors. Published by Wiley-VCH Verlag GmbH & Co. KGaA. This is an open access article under the terms of the Creative Commons Attribution Non-Commercial License, which permits use, distribution and reproduction in any medium, provided the original work is properly cited and is not used for commercial purposes.

mately 575 nm, B-term scattering dominates,[7] which involves vibronic coupling between two allowed excited electronic transitions. Early studies on metalloporphyrins in solution showed that both $Q_0$ and $Q_v$ bands are predominantly governed by the strong Herzberg–Teller coupling of antisymmetric $A_{2g}$ modes,[8,9] providing evidence of vibronic coupling. Enhancement with 514.5 and 532 nm excitation laser lines, which are in close proximity to the vibronic $Q_v$ band of the visible spectrum of hemoporphyrins,[10] enables the C-term enhancement mechanism to dominate,[11] which occurs between forbidden electronic transitions that are prohibited at the equilibrium geometry of the molecule.[6] As is the case for $Q_0$, RR spectra obtained by exciting into the $Q_v$ contain polarized, depolarized, and anomalous polarized bands and lead to additional enhancement of non-fundamental modes.[8,12]

The overtones and combination bands in the RR spectra of some metalloporphyrins have previously been reported based on polarization measurements.[13-16] The use of 514.5 nm excitation gave the strongest enhancement of non-fundamental bands in porphyrins compared to other excitation lines,[13] because of C-term scattering.

Previously, the observation of overtones and combination modes in the RR spectra were attributed to strong electron–nuclear coupling in such species.[17,18] Strong intermolecular coupling was explained by multichromophore interactions that occur in a protein reaction center.[19] Such interactions were invoked for bacteriochlorophyll where the structural arrangement of the chromophores enables enhancement in the vicinity of the $Q_v$ transition.[19] A quantitative description of the scattering processes with transform theory was suggested, in which electron–nuclear coupling strengths are proportional to the intensity ratio of the overtone and fundamental region.[17]

It was further postulated that heme proteins such as Hb fall into the category of weak coupling compounds, because the electronic transitions of these compounds are distributed over several nuclei.[7,17] Strekas and Spiro reported that, although RR spectra sometimes display intense overtone progressions, these are not apparent in the RR spectra of Hb.[20] It is important to note that these early reports were based on what was known from solution-phase studies.

Here, we report the appearance of overtone and combination bands for Hb in red blood cells (RBCs) and crystalline deposits, but not in solutions. This suggests that the structural arrangement of Hb inside single RBCs (highly aligned) may be responsible for a significant increase in the non-fundamental modes in the vibronic $Q_v$ side band. We demonstrate that by incorporating the non-fundamental region into a partial least-squares discriminant analysis (PLS-DA) model improves the diagnostic capability of the Raman technique for malaria compared to analyzing the fundamental region alone. Moreover, the bands associated with oxyHb in malaria-infected RBCs can be identified more readily in the non-fundamental region because of the intense overlapping hemozoin bands, which obscure the oxyHb bands in the fundamental region.

## 2. Results and Discussion

The most interesting observation drawn from the comparison of the spectra presented in Figure 2 is the extraordinary spectral profile in the higher spectral region (3200–2300 $cm^{-1}$)

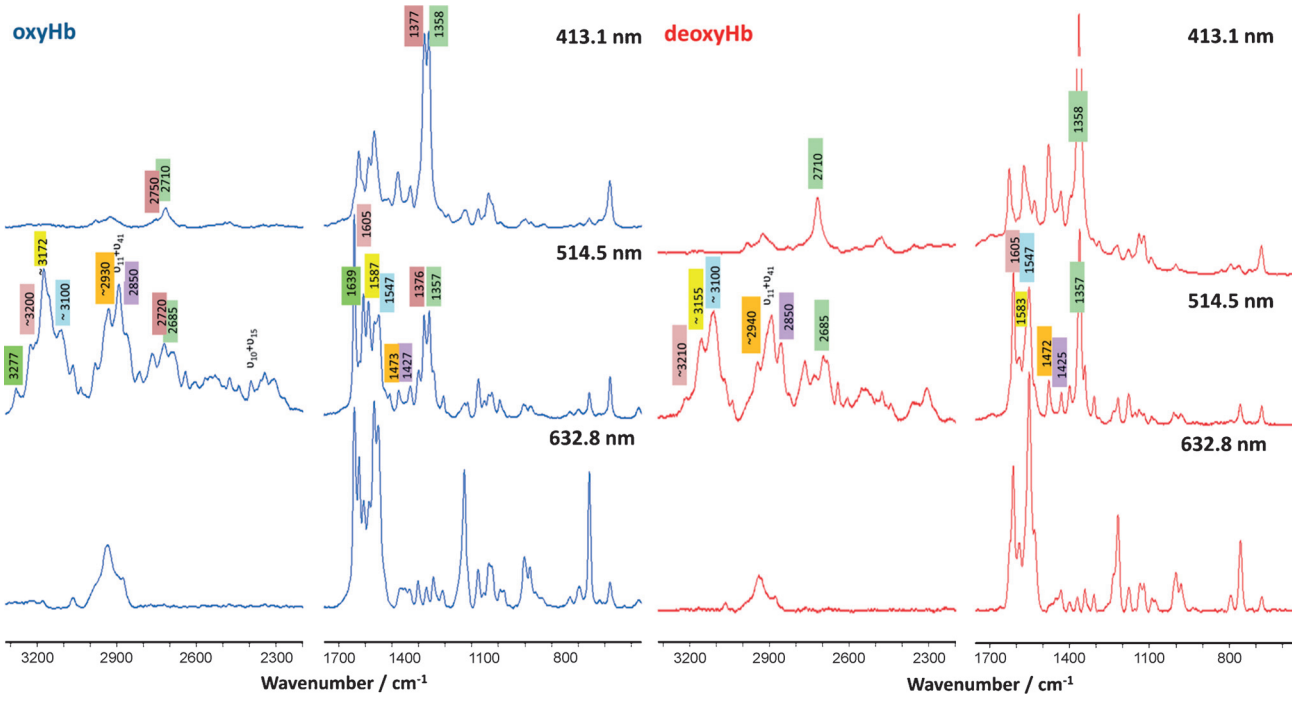



**Figure 2.** Comparison between average RR spectra collected from ten different oxygenated and deoxygenated RBCs, obtained by using 413.1, 514.5, and 632.8 nm laser wavelengths in the spectral regions of 3300–2200 $cm^{-1}$ and 1700–600 $cm^{-1}$. The color assignments of the fundamental bands have corresponding colors for their respective overtones. The intensity of the bands in the 3300–2200 $cm^{-1}$ have not been scaled or normalized and appear on the same scale as the fundamental region.

© 2014 The Authors. Published by Wiley-VCH Verlag GmbH & Co. KGaA, Weinheim

when applying 514.5 nm excitation. RR spectra of RBCs in this region obtained with the use of 413.1 and 514.5 nm excitation show bands that are non-typical for protein aliphatic and aromatic stretching vibrations. These modes appear hyper-enhanced when using 514.5 nm excitation and many are more intense than their associated fundamentals. Moreover, this region clearly differs amongst spectra obtained of oxyHb and deoxyHb inside RBCs. The most crucial observation is that the most intense bands in the higher wavenumber region, corresponding to the first overtone bands, are directly correlated to the most intense bands in the fundamental region.

The bands in the region of 3100–2800 $cm^{-1}$ for RR spectra of both oxyHb and deoxyHb obtained with 632.8 nm excitation do not differ in wavenumber values and are typical for CH, $CH_2$, and $CH_3$ groups of proteins.[21]

Exciting RBCs with 413.1 nm radiation revealed two intense oxidation-state marker bands at 1377 and 1358 $cm^{-1}$ in the oxyHb spectrum, whereas in the deoxyHb spectrum, only one band with higher intensity (ca. three times higher) at 1358 $cm^{-1}$ was observed. These fundamental marker bands of the oxidation state ($\nu_4$) have overtones, which mimic the behavior of their fundamental counterparts. The RR band at 2720 $cm^{-1}$ was previously assigned to an overtone of the $\nu_4$ mode ($2\nu_4$) for cytochrome C,[17] measured with 413.1 nm excitation. Therefore, overtones observed at 2710 $cm^{-1}$, with a shoulder at 2750 $cm^{-1}$, can be used as marker bands for oxygenated RBCs (low spin, $Fe^{3+}$). The observation of the single overtone at 2710 $cm^{-1}$ with higher intensity corresponds to deoxygenated RBCs (high spin, $Fe^{2+}$). The fact that both ferric and ferrous bands appear in the spectra of oxyHb RBCs indicates that the cell was either only partially oxygenated or some laser induced photodissociation of the oxyHb was occurring. Nonetheless, this highlights the sensitivity of the overtones to oxidation induced perturbation of the heme core.

The excitation of live RBCs with the 514.5 nm laser wavelength results in highly intense numerous overtones compared to 413.1 and 632.8 nm. Parallel ($I_{||}$) and perpendicular ($I_{\perp}$) polarization components enabled the vibrational assignment of the overtones and combination modes of the most intense fundamental bands (Figure 3). In the fundamental region of oxyHb and deoxyHb RBCs, the strongest bands are present in the spectral region of 1700–1200 $cm^{-1}$ and, therefore, the overtones or combinations appear in the 3200–2300 $cm^{-1}$ region. Detailed assignments are shown in Table S1 (in the Supporting Information) based on previous studies on model porphyrin compounds.[3,18,20,22–26]

The assigned symmetry species for the non-fundamental modes are based on the work by Kitagawa et al.[13] By symmetry, all overtones are assigned to $A_{1g}$ modes. In terms of the intensities of the bands in the spectral region of 3200–2200 $cm^{-1}$ of RBCs, the parallel ($I_{||}$) polarization component exhibits a much higher intensity than the perpendicular ($I_{\perp}$) polarization components, indicating the bands observed in the higher region are polarized and are, therefore, assigned to overtones or combination bands of the same symmetry modes, simplifying the band assignment.

The bands characteristic of oxyHb that appear at 1639, 1605, 1587, 1547, and 1473 $cm^{-1}$ originate from $\nu_{10}$, $\nu_{19}$, $\nu_{37}$, $\nu_{11}$, and $\nu_3$ porphyrin stretching modes, respectively. The band at around 1640 $cm^{-1}$, assigned to $\nu_{10}$, may be treated as a marker

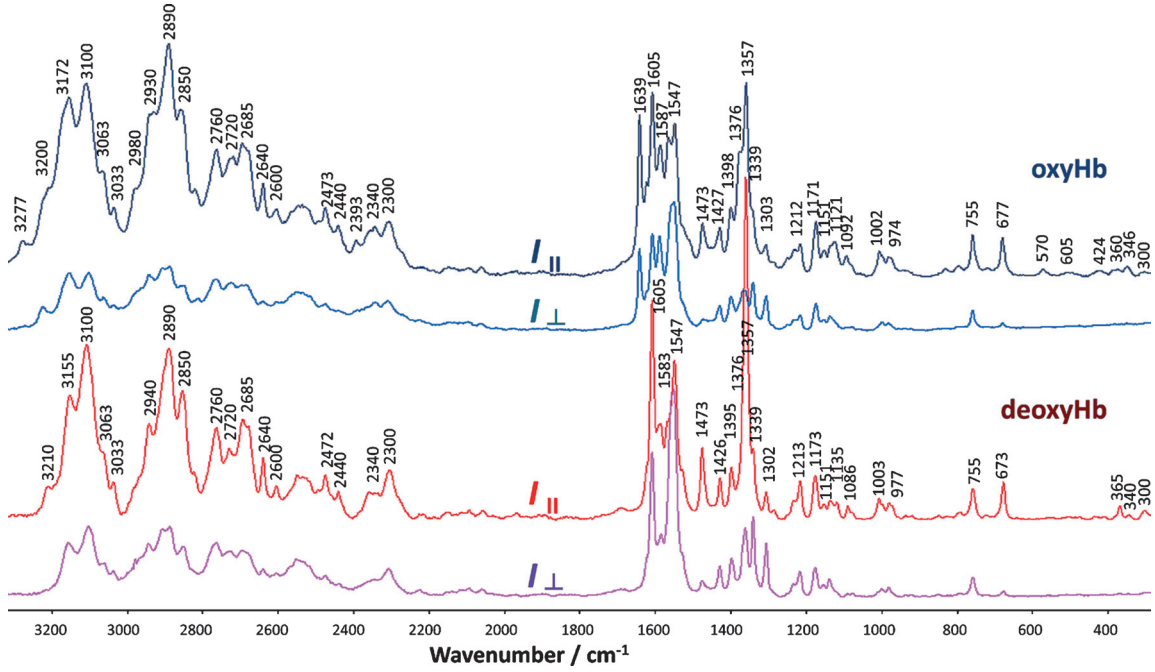



**Figure 3.** The average RR spectra collected from ten different oxygenated and deoxygenated functional RBCs, obtained with 514.5 nm laser excitation in the 3300–250 $cm^{-1}$ spectral region. The top (dark blue, red) and bottom (light blue, pink) spectra represent the parallel ($I_{||}$) and perpendicular ($I_{\perp}$) polarization components, respectively.

© 2014 The Authors. Published by Wiley-VCH Verlag GmbH & Co. KGaA, Weinheim

for oxyHb.[20] The in-plane translocation of the Fe atom in oxyHb causes the intensity of $\nu_{10}$ to increase and is typical for low-spin Hb derivatives. The overtone of this marker band for oxyHb band is observed at 3277 $cm^{-1}$ and is not observed in the overtone region of deoxyHb.

The band at 1587 $cm^{-1}$, assigned to $\nu_{37,}$ is more intense for oxyHb and shifts to 1583 $cm^{-1}$ in deoxyHb. The shift of approximately 4 $cm^{-1}$ in the fundamental region increases to a shift of 17 $cm^{-1}$ between overtones of these two bands for the oxyHb and deoxyHb spectra. Moreover, the intensity of the overtone of the $\nu_{37}$ for oxyHb observed at 3172 $cm^{-1}$ has a much higher intensity than the corresponding band in deoxyHb observed at around 3155 $cm^{-1}$. Furthermore, the intensity of the overtone at 3172 $cm^{-1}$ decreases with increasing laser power. Other bands exhibited similar behavior at higher laser power, indicating photodissociation of oxyHb. Interestingly this photodissociation could be directly followed by RR spectroscopy in the overtone region as clearly as the fundamental region.

The hyper-enhanced overtone region enables the generation of Raman images of single cells (Figure S1). In this case, a 532 nm laser confocal-imaging microscope was used to generate the images, as our 514.5 nm microscope system is not set up for imaging and, hence, the overtones are not quite as intense as they would be at 514.5 nm. Nonetheless, most of the overtone bands still have very strong intensity, enabling high-contrast images to be generated. This is the first example of a Raman image based on the integrated intensity from an overtone band for any cell.

7To determine if the intense overtones are observed in other heme species, we investigated the solid-state spectra of a number of heme derivatives including Hb Ao, hematin, ferric octaethylporphyrins, and methylporphyrin complexes (Figure S2). Like RBCs, these molecules also show a rich non-fundamental spectrum when exciting with 514.5 nm excitation, indicating that this phenomena is observed for all solid-state hemes. However, the non-fundamental region for standard compounds of hemoglobin Ao has a lower intensity of the overtone and combination bands compared to functional RBCs. The qualitative ratios ($I_{overtone}/I_{fundamental}$) for an average oxyHb spectrum obtained from ten different functional RBCs for the main modes $\upsilon_{10,}$ $\upsilon_{37,}$ $\upsilon_{4,}$ and $\upsilon_{19}$ are equal to 0.16, 0.53, 0.95, and 0.5, respectively. The intensity ratios ($I_{overtone}/I_{fundamental}$) for a solid sample of Hb, which was submerged in distilled water and measured with the use of the same immersive objective as RBCs, are equal to 0.14, 0.48, 0.84, and 0.33. Extensive enhancement of the totally symmetric modes was observed with 830 nm excitation in the spectrum of Fe(OEP)Cl (OEP = octaethylporphyrin), well away from the Soret band (~400 nm) where these modes are normally enhanced. The enhancement of totally symmetric modes in the near-IR region was attributed to excitonic interactions occurring in the heme array.[27]

It is important to note that even very saturated solutions of Hb and heme derivatives do not show enhanced non-fundamental modes. These modes are only observed in RBCs (where the concentration of Hb is on the order of 22 mM),[28] in crystals, and in amorphous heme aggregates. This indicates that there is an extra enhancement mechanism at play in the case of RBCs, which is evident when measuring the parallel polarized light component.

This mechanism may be understood in terms of aggregated enhanced Raman scattering (AERS) where molecular excitons result from the resonance interaction between the excited states of loosely bound molecular aggregates.[29] AERS has previously been used to explain the dramatic enhancement of fundamental modes observed in the RR spectra of porphyrins,[30] cyano dyes,[31] Hb in RBCs,[32] and hemozoin (malaria pigment).[33,34] Akins[35] coined the term AERS to describe unusual scattering in small aggregates of covalently linked porphyrin arrays and cyanine dyes absorbed onto surfaces. He proposed a theoretical description and experimentally demonstrated that an increase in the number of aggregated chromophores produces near-resonance of both the A and B terms in the polarizability tensor.

Previously, it has been demonstrated that the orientation of the RBC dictates the type of enhancement pattern observed in the RR spectrum.[36] It appears that the RBC behaves like a light polarizer, preferentially scattering perpendicular and parallel light depending on the orientation of the cell. Moreover, we have shown that the UV/Vis spectra of RBCs exhibit shifting and broadening of the Soret band, which is also indicative of excitonic interactions.[32] The fact that the enhancement of both fundamentals and overtones is far more dramatic in a single cell than in an isolated crystal of Hb points to a high degree of alignment and ordering in the RBC conducive to an excitonic mechanism.

The incorporation of the non-fundamental region into a PLS-DA model allowed us to improve the malaria diagnostic capability of the Raman technique. Figure 4 presents cross-validation errors for the PLS-DA model performed on functional RBCs containing malaria trophozoites and non-infected RBCs (control), using the whole (Figure 4a) and the fundamental region (Figure 4b). The importance of the non-fundamental region on the discrimination is evident in the variable importance in projection (VIP) scores.[34] A VIP score close to or greater than 1 is considered to be important in the given model. As can be seen in Figure 4C, the hyper-intense non-fundamental region has a strong impact on the model, with VIP values higher than those of the fundamental modes, with the exception of the strong 1600–1500 $cm^{-1}$ bands that are mainly associated with porphyrin C=C stretching modes.

A comparison of the RR spectra of hemozoin, the control, and *P. falciparum*-infected RBCs demonstrates another application of the non-fundamental region. Figure S3 shows that, in the case of malaria-parasite-infected RBCs, the fundamental region of the spectrum is dominated by hemozoin bands, which almost totally obscure the oxyHb bands, whereas the non-fundamental region of the spectrum is dominated by oxyHb bands. Consequently, it is possible to obtain information about the relative contribution of hemozoin and oxyHb. It has been reported that the malaria infection leads to a decreased 2,3-biphosphoglycerate (2,3-BPG) concentration, which, in turn, lowers the concentration of oxyHb in bulk-infected RBCs.[37] Our method allows the detection of a relative

© 2014 The Authors. Published by Wiley-VCH Verlag GmbH & Co. KGaA, Weinheim

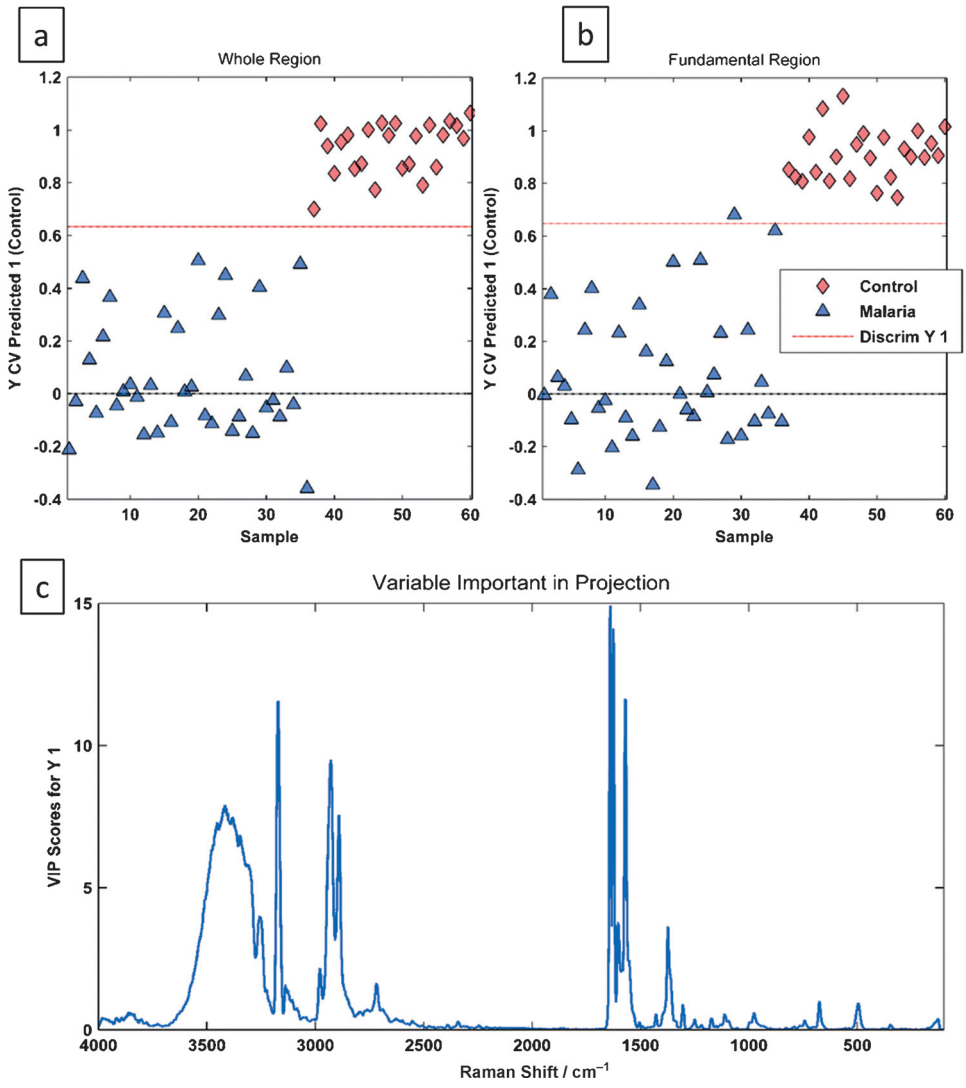



**Figure 4.** Cross-validation errors for the PLS-DA performed on the evaluation of the discrimination capability between the control (non-infected RBCs) and malaria (infected RBCs) samples, using the whole (a) and the fundamental (b) regions. Variable importance in projection for the PLS-DA performed on the whole region (c).

amount of hemozoin and oxyHb in individual RBCs infected with *P. falciparum*. This will prove very useful for future Raman-based malaria diagnostic methods.

## 3. Conclusions

The intensity and richness of the Hb spectrum at 514.5 nm, both in the fundamental and non-fundamental regions, has the potential to improve the diagnostic and monitoring capability of Raman-based medical devices, particularly in diseases such as malaria and other hemopathies because the number of extra bands and their intensity will provide a more detailed molecular fingerprint.

## Experimental Section

Fresh blood (20 μL) from healthy volunteers was diluted with cold saline solution (10 mL) and measured as previously described.[32] To prepare the deoxygenated RBCs, the saline solution was equilibrated with gaseous $N_2$. The 3D7 strain of *Plasmodium falciparum* was used in this study and cultured, essentially, as previously described.[38] Trophozoite-stage parasites were enriched from cultures by Percoll purification, as described previously.[39]

The power of the laser at the sample position for all Raman measurements was $\leq$0.5 mW, and the beam was slightly defocused on the RBCs to prevent localized heating, which prevented photo/thermal degradation of heme aggregates in RBCs.[32,38] Raman measurements of the RBCs were recorded by using a Renishaw System 2000 instrument with 632.8, 413.1, and 514.5 nm excitation laser lines. The spectra were recorded in the region of 3500–100 $cm^{-1}$ with spectral resolution of 1 $cm^{-1}$. Each spectrum was recorded from a different RBC and one scan was acquired for each cell with a laser exposure time of 10 s. The spectra of oxyHb and deoxyHb from live RBCs were averaged from 20 individual Raman spectra obtained from 20 different cells. Polarization measurements were performed by using 514.5 nm excitation with a polarizer filter for the parallel component and a combination of a polarizer filter and half-wave plate for the perpendicular component. For single measurements, a water-immersive Olympus (×60/0.90 NA) objective was used. Raman data analysis was performed with Opus and WITec software. The average UV/Vis electronic absorption spectra of oxyHb and deoxyHb were recorded from the 4×4 μm cell surface area of ten single functional RBCs in the spectral region of 300–650 nm by using a UV/Vis spectrophotometer (MSP 210 Microscope Spectrometry System, J&M Analytische Mess- und Regeltechnik GmbH) and a 60× immersion objective. A detailed description of the methods is presented in the Supporting Information.

## *Acknowledgements*

*B.R.W. is supported by an Australian Research Council (ARC) Future Fellowship (FT120100926) and the instrument was purchased through an ARC Linkage Infrastructure Equipment and Facilities (LEIF) grant (LE100100215). This work is supported, in part, by an ARC grant DP140102504 and by the European Union from the resources of the European Regional Development Fund under the Innovative Economy Program (Grant coordinated by JCET-UJ, No. POIG.01.01.02–00–069/09). K.M.M. acknowledges fi-*

© 2014 The Authors. Published by Wiley-VCH Verlag GmbH & Co. KGaA, Weinheim

*nancial support from a Go8 Fellowship, enabling a research stay at Monash University and the Polish National Science Center (NCN) (grant no. UMO-2012/07/D/ST4/02214). D.P.G. acknowledges financial support from the grant "Segles V" provided by the University of Valencia, enabling a research stay at Monash University. We thank Finlay Shanks (Monash University) for instrumental support.*

**Keywords:** malaria diagnostic · overtone/combination modes · porphyrinoids · Raman spectroscopy · red blood cells

[1] T. G. Spiro, T. C. Strekas, *Proc. Natl. Acad. Sci. USA* **1972**, *69*, 2622 – 2626.
[2] V. Jayaraman, R. Kenton, I. Mukerji, T. G. Spiro, *Science* **1995**, *269*, 1843 – 1848.
[3] B. R. Wood, D. McNaughton, *J. Raman Spectrosc.* **2002**, *33*, 517 – 523.
[4] T. C. Strekas, A. J. Packer, T. G. Spiro, *J. Raman Spectrosc.* **1973**, *1*, 197 – 206.
[5] S. Nagatomo, M. Nagai, T. Kitagawa, *J. Am. Chem. Soc.* **2011**, *133*, 10101 – 10110.
[6] S. A. Asher, *Annu. Rev. Phys. Chem.* **1988**, *39*, 537 – 588.
[7] J. Wang, S. Takahashi, D. L. Rousseau, *Proc. Natl. Acad. Sci. USA* **1995**, *92*, 9402 – 9406.
[8] F. Paulat, V. K. K. Praneeth, C. Näther, N. Lehnert, *Inorg. Chem.* **2006**, *45*, 2835 – 2856.
[9] M. Levantino, Q. Huang, A. Cupane, M. Laberge, A. Hagarman, R. Schweitzer-Stenner, *J. Chem. Phys.* **2005**, *123*, 054508.
[10] J. R. Ferraro, K. Nakamoto, Introductory Raman Spectroscopy, Academic Press Inc., San Diego, **1994**.
[11] J. Tang, A. C. Albrecht in *Raman Spectroscopy* (Ed.: H. A. Szymanski), Plenum Press, New York, **1970**.
[12] R. S. Czernuszewicz, T. G. Spiro in *Inorganic electronic structure and spectroscopy* (Eds.: E. I. Solomon, A. B. P. Lever) Wiley & Sons, New York, **1999**, pp. 353 – 441.
[13] T. Kitagawa, M. Abe, H. Ogoshi, *J. Chem. Phys.* **1978**, *69*, 4516 – 4525.
[14] S. Mendelsohn, S. Sunder, A. L. Verma, H. J. Bernstain, *J. Chem. Phys.* **1975**, *62*, 37 – 44.
[15] S. Sunder, S. Mendelsohn, H. J. Bernstain, *Biochem. Biophys. Res. Commun.* **1975**, *62*, 12 – 16.
[16] J. M. Friedman, R. M. Hochstrasser, *J. Am. Chem. Soc.* **1976**, *98*, 4043 – 4048.
[17] Y. Gu, P. M. Champion, *Chem. Phys. Lett.* **1990**, *171*, 254 – 258.
[18] M. Abe, T. Kitagawa, Y. Kyoguku, *J. Chem. Phys.* **1978**, *69*, 4526 – 4534.
[19] L. D. Book, A. E. Ostafin, N. Ponomarenko, J. R. Norris, N. F. Scherer, *J. Phys. Chem. B* **2000**, *104*, 8295 – 8307.
[20] T. C. Strekas, T. G. Spiro, *Biochim. Biophys. Acta.* **1972**, *263*, 830 – 833.
[21] N. K. Howell, G. Arteaga, S. Nakai, E. C. Li-Chan, *J. Agric. Food Chem.* **1999**, *47*, 924 – 33.
[22] H. Okamoto, S. Saito, H. Hamaguchi, M. Tasumi, C. H. Eugster, *J. Raman Spectrosc.* **1984**, *15*, 331 – 335.
[23] T. G. Spiro, T. C. Strakes, *J. Am. Chem. Soc.* **1974**, *96*, 338 – 345.
[24] A. Rygula, K. Majzner, K. M. Marzec, A. Kaczor, M. Pilarczyk, M. Baranska, *J. Raman Spectrosc.* **2013**, *44*, 1061 – 1076.
[25] M. Ogawa, Y. Harada, Y. Yamaoka, K. Fujita, H. Yaku, T. Takamatsu, *Biochem. Biophys. Res. Commun.* **2009**, *382*, 370 – 374.
[26] T. Kitagawa, Y. Kyogoku, T. Iizuka, M. I. Saito, *J. Am. Chem. Soc.* **1976**, *98*, 5169 – 5173.
[27] R. Puntharod, G. T. Webster, M. Asghari-Khiavi, K. R. Bambery, F. Safinejad, S. Rivadehi, S. J. Langford, K. J. Haller, B. R. Wood, *J. Phys. Chem. B* **2010**, *114*, 12104 – 12115.
[28] W. J. Williams, E. Beutler, A. Erslev, M. A. Lichtman, *Hemotology*, 3 rd edition, McGraw-Hill: New York, **1983**.
[29] M. Kasha, *Radiat. Res.* **1963**, *20*, 55 – 71.
[30] D. L. Akins, S. Özçelik, H.-R. Zhu, C. Guo, *J. Phys. Chem. A* **1997**, *101*, 3251 – 3259.
[31] D. L. Akins in *J-Aggregates* (Ed.: T. Kobayashi), World Scientific, New Jersey, **1996**, pp. 67 – 94.
[32] B. R. Wood, L. Hammer, L. Davis, D. McNaughton, *J. Biomed. Opt.* **2005**, *10*, 014005.
[33] B. R. Wood, S. J. Langford, B. M. Cooke, J. Lim, F. K. Glenister, M. Duriska, J. K. Unthank, D. McNaughton, *J. Am. Chem. Soc.* **2004**, *126*, 9233 – 9239.
[34] B. R. Wood, A. Hermelink, P. Lasch, K. R. Bambery, G. T. Webster, M. Asghari-Khiavi, B. M. Cooke, S. Deed, D. Naumann, D. McNaughton, *Analyst* **2009**, *134*, 1119 – 1125.
[35] D. L. Akins, *J. Phys. Chem.* **1986**, *90*, 1530 – 1534.
[36] B. R. Wood, L. J. Hammer, D. McNaughton, *Vibr. Spectrosc.* **2005**, *38*, 71 – 78.
[37] W. Schmidt, R. Correa, D. Boning, J. H. H. Ehrich, C. Kruger, *Blood* **1994**, *83*, 3746 – 3752.
[38] M. Foley, L. W. Deady, K. Ng, A. F. Cowman, L. Tilley, *J. Biol. Chem.* **1994**, *269*, 6955 – 6961.
[39] A. Knight, R. E. Sinden, *Trans. R. Soc. Trop. Med. Hyg.* **1982**, *76*, 503 – 509.

Received: August 22, 2014
Published online on September 26, 2014

© 2014 The Authors. Published by Wiley-VCH Verlag GmbH & Co. KGaA, Weinheim